

Thermalization time in many-body quantum systems

Talía L. M. Lezama,¹ E. Jonathan Torres-Herrera,² Francisco Pérez-Bernal,³ Yevgeny Bar Lev,¹ and Lea F. Santos⁴

¹*Department of Physics, Ben-Gurion University of the Negev, Beer-Sheva 84105, Israel*

²*Instituto de Física, Benemérita Universidad Autónoma de Puebla, Apt. Postal J-48, Puebla, 72570, Mexico*

³*Dep. CC. Integradas y Centro de Estudios Avanzados en Física,*

Matemáticas y Computación. Fac. CC. Experimentales, Universidad de Huelva, Huelva 21071,

& Instituto Carlos I de Física Teórica y Computacional, Universidad de Granada, Granada 18071, Spain

⁴*Department of Physics, Yeshiva University, New York, New York 10016, USA*

Isolated chaotic many-body quantum systems can reach thermal equilibrium, but it is not yet clear how long they take to do so. To answer this question, we use exact numerical methods and analyze the entire evolution, from perturbation to thermalization, of a paradigmatic disordered many-body quantum system in the chaotic regime. We investigate how the thermalization time depends on the system size and observables. We show that if dynamical manifestations of spectral correlations in the form of the correlation hole (“ramp”) are taken into account, the time for thermalization scales exponentially with system size, while if they are neglected, the scaling is better described by a power law with system size, though with an exponent larger than expected for diffusive transport.

I. INTRODUCTION

One major question in studies of nonequilibrium dynamics of isolated many-body quantum systems is how long it takes for an experimentally relevant observable to reach equilibrium, that is, to reach a point beyond which its expectation value simply fluctuates around its infinite-time average and the size of these fluctuations decreases as the system size increases [1–6]. Equilibration in this sense does not necessarily imply thermalization.

The variety of approaches taken to address this question and the lack of agreement among the existing results are worrisome. Several analyses are based on assumptions about the spectrum, observables, and initial conditions, and often provide bounds for the equilibration time. Some suggest that this time should decrease with system size [7, 8], others that it should depend weakly on it [9], and others yet that it should increase with it [3, 4, 10–16], possibly exponentially [7, 17]. Studies aligned with transport behavior [18–31], on the other hand, expect the equilibration time to increase as a power law with system size.

Confronted by so many options, it is worth to step back and try first to identify a general scenario. For this purpose, we focus specifically on the time for thermalization, examining many-body quantum systems that are in the chaotic regime. In this case, initial states far from equilibrium and with energy expectation values away from the edges of the many-body spectrum lead to thermal equilibrium [32–34]. This allows us to avoid the particularities of integrable models and specific initial states.

The largest possible timescale in quantum systems is given by the inverse of their mean-level spacing, the so-called Heisenberg time, which grows linearly with the dimension of the Hilbert space, and thus exponentially with system size. The Heisenberg time is the absolute upper bound for the thermalization time, but do experimental observables take this long to thermalize? This is the main question addressed by this work. The answer is yes [35] if the dynamical manifestations of spectral correlations, known as correlation hole [35–42] and sometimes referred to as “ramp” [43–45], are taken into account. However, as we show here, these manifestations can be neglected for some observables, leading instead to a power-law scaling of the thermalization time with system size, a result that is in better agreement with studies of transport behavior [31, 34].

We investigate the evolution of the survival (return) probability, which is the probability of finding the system in its initial state later in time and may be accessible to experiments with cold atoms [46, 47]; the inverse participation ratio, which quantifies the spreading in time of the initial state over the many-body Hilbert space and whose logarithm gives the participation second-order Rényi entropy; the spin autocorrelation function, which is related to the imbalance measured in experiments with cold atoms [48]; and the connected spin-spin correlation function measured in experiments with ion traps [49]. Our analysis focuses on the disordered spin-1/2 Heisenberg chain in the chaotic regime and we briefly discuss the dependence of the thermalization time on disorder strength.

The article is organized as follows. Section II introduces the disordered model, initial conditions, and observables. In Sec. III, we show the timescales for the correlation hole and for the thermalization after it. In Sec. IV, the correlation hole is neglected and a new definition for the thermalization time is proposed. Its dependence on the disorder strength is also provided. Conclusions are presented in Sec. V.

II. MODEL, INITIAL STATES, AND OBSERVABLES

A. Model

The disordered spin-1/2 Heisenberg chain that we consider is a representative model of disordered interacting one-dimensional systems and has been extensively used in studies of many-body localization [50–53]. It is given by the following Hamiltonian,

$$\hat{H} = \sum_{i=1}^L J \hat{\mathbf{S}}_i \cdot \hat{\mathbf{S}}_{i+1} + h_i \hat{S}_i^z, \quad (1)$$

where $\hat{\mathbf{S}}_i \equiv (\hat{S}_i^x, \hat{S}_i^y, \hat{S}_i^z)$ are spin-1/2 operators, L is the system size, periodic boundary conditions are assumed, we set $J = 1$ and h_i to be independent and uniformly distributed random variables in $[-W, W]$, with W being the onsite disorder strength. The system conserves the total magnetization in the z -direction, $\hat{S}_{\text{tot}}^z = \sum_i^L \hat{S}_i^z$, and exhibits a transition to the many-body localized phase at a critical disorder strength of W_c . The value of W_c is still under debate [54–63], some papers estimate that $3 < W_c < 4$ and others that $W_c > 4$.

We work in the $\hat{S}_{\text{tot}}^z = 0$ subspace that has the Hilbert space dimension $D = \binom{L}{L/2}$, and consider finite systems away from the critical region, $0.5 \leq W \lesssim 1$, although a short discussion for values of disorder closer to the critical region $1 < W < 3$ is also provided.

B. Initial states and thermalization

We use initial states $|\Psi(0)\rangle$ that are product states in the S^z -basis, $|\phi_n\rangle$, such as $|\uparrow\downarrow\downarrow \dots \uparrow\rangle$, which can be experimentally realized. We choose initial states with an energy expectation value $\langle\Psi(0)|\hat{H}|\Psi(0)\rangle$ far from the edges of the spectrum to guarantee that they fall in the chaotic region of the many-body Hamiltonian and that a given few-body observable \hat{O} reaches thermal equilibrium. Its infinite-time average expressed in terms of the many-body eigenstates $\hat{H}|\alpha\rangle = E_\alpha|\alpha\rangle$ is given by

$$\bar{O} = \sum_{\alpha} |C_{\alpha}|^2 \langle\alpha|\hat{O}|\alpha\rangle, \quad (2)$$

where $C_{\alpha} \equiv \langle\alpha|\Psi(0)\rangle$.

We use either exact diagonalization or Krylov-space methods to evolve the system in time. All results are averaged over 10^4 samples composed of $0.01D$ initial states and $10^4/(0.01D)$ disorder realizations. The average over samples is denoted by the angle brackets $\langle\cdot\rangle$. We have also verified that fixing a single initial state and using 10^4 disorder realizations leads to equivalent results, though the numerical procedure is less efficient. All statistical errors are accessed using a bootstrap procedure.

C. Observables

We study the time-evolution of two non-local (in real space) observables, the survival probability and the inverse participation ratio, and two local quantities, the spin autocorrelation function and the connected spin-spin correlation function.

1. Non-local Quantities

The survival probability is defined as

$$P_S(t) = |\langle\Psi(0)|\Psi(t)\rangle|^2. \quad (3)$$

Taking the mean gives,

$$\langle P_S(t) \rangle = \left\langle \sum_{\alpha \neq \beta} |C_{\alpha}|^2 |C_{\beta}|^2 e^{-i(E_{\alpha} - E_{\beta})t} \right\rangle + \left\langle \sum_{\alpha} |C_{\alpha}|^4 \right\rangle, \quad (4)$$

which is related to the spectral form factor, $\langle \sum_{\alpha \neq \beta} e^{-i(E_\alpha - E_\beta)t} \rangle$. While $\langle P_S(t) \rangle$ is a true dynamical quantity, which depends on the initial state through the components C_α , the spectral form factor involves only the eigenvalues of the Hamiltonian and is used to study the manifestation of level statistics in the time domain [64]. Filter functions are sometimes added to it [45, 65], but they do not come from the quench dynamics, as the coefficients C_α in $\langle P_S(t) \rangle$.

The second non-local quantity that we consider is the inverse participation ratio,

$$\text{IPR}(t) = \sum_n |\langle \phi_n | \Psi(t) \rangle|^4, \quad (5)$$

which measures the spreading in time of the initial state $|\Psi(0)\rangle$ over the many-body Hilbert space. Its logarithm, $-\ln \text{IPR}(t)$, corresponds to the second-order Rényi entropy.

2. Local Observables

The spin autocorrelation function measures the proximity of the spin configuration in the z -direction at a time t to the initial spin configuration,

$$\mathcal{I}(t) = \frac{4}{L} \sum_{i=1}^L \langle \Psi_0 | \hat{S}_i^z(0) \hat{S}_i^z(t) | \Psi_0 \rangle, \quad (6)$$

where $\hat{S}_i^z(t) = e^{iHt} \hat{S}_i^z(0) e^{-iHt}$. For the Néel initial state, $|\uparrow\downarrow\uparrow\downarrow\uparrow\downarrow\dots\rangle$, it reduces to the density imbalance between even and odd sites that is measured in experiments with cold atoms [48].

The connected spin-spin correlation function is defined as

$$C(t) = \frac{4}{L} \sum_{i=1}^L \left[\langle \Psi(t) | \hat{S}_i^z \hat{S}_{i+1}^z | \Psi(t) \rangle - \langle \Psi(t) | \hat{S}_i^z | \Psi(t) \rangle \langle \Psi(t) | \hat{S}_{i+1}^z | \Psi(t) \rangle \right] \quad (7)$$

and has been measured in experiments with ion traps [49].

III. THERMALIZATION AFTER THE CORRELATION HOLE

A semi-analytical expression for the entire evolution of the average of the survival probability was derived for realistic chaotic many-body quantum systems with short-range interactions [35, 42], as the one described by Eq. (1), and it is given by

$$\langle P_S(t) \rangle = \frac{1 - \langle \overline{P_S} \rangle}{(D-1)} \left[D b_1^2(\Gamma t) - b_2 \left(\frac{\Gamma t}{\sqrt{2\pi D}} \right) \right] + \langle \overline{P_S} \rangle, \quad (8)$$

where

$$\Gamma^2 = \langle \Psi(0) | \hat{H}^2 | \Psi(0) \rangle - \langle \Psi(0) | \hat{H} | \Psi(0) \rangle^2 \quad (9)$$

is the squared width of the energy distribution of the initial state, $\langle \overline{P_S} \rangle$ is the mean of the infinite-time average of $P_S(t)$,

$$b_1^2(\Gamma t) = \frac{e^{-\Gamma^2 t^2}}{4\mathcal{N}^2} \left| \text{erf} \left(\frac{E_{\max} + it\Gamma^2}{\sqrt{2}\Gamma} \right) - \text{erf} \left(\frac{E_{\min} + it\Gamma^2}{\sqrt{2}\Gamma} \right) \right|^2, \quad (10)$$

\mathcal{N} is a normalization constant, erf is the error function, E_{\max} and E_{\min} are the largest and smallest eigenvalues of \hat{H} , respectively, and

$$b_2(t) = \begin{cases} 1 - 2t + t \ln(2t + 1) & t \leq 1 \\ t \ln \left(\frac{2t + 1}{2t - 1} \right) - 1 & t > 1, \end{cases} \quad (11)$$

is the two-level form factor.

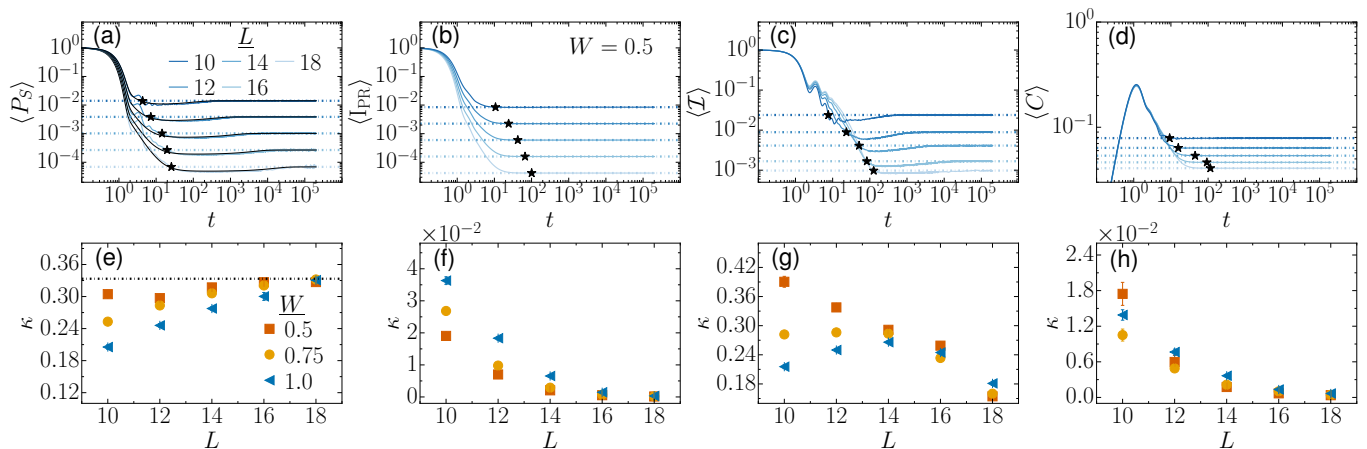


FIG. 1. *Upper panels*: Time evolution of the mean (a) survival probability $\langle P_S(t) \rangle$, (b) inverse participation ratio $\langle I_{PR}(t) \rangle$, (c) spin autocorrelation function $\langle \mathcal{I}(t) \rangle$, and (d) connected spin-spin correlation function $\langle C(t) \rangle$ for different system sizes, as indicated in panel (a), and for disorder strength $W = 0.5$, as shown in panel (b). The horizontal dotted-dashed lines mark the asymptotic values and the stars indicate the crossing time t^* . In Fig. 1 (a), the numerical data overlap with the curves for the semi-analytical expression in Eq. (8). *Lower panels*: Relative depth of the correlation hole, κ , as a function of L , for (e) $\langle P_S(t) \rangle$, (f) $\langle I_{PR}(t) \rangle$, (g) $\langle \mathcal{I}(t) \rangle$, and (h) $\langle C(t) \rangle$ for three values of the disorder strength in the chaotic regime, as indicated in Fig. 1 (e). The horizontal dashed line in panel (e) corresponds to the value $\kappa = 1/3$ obtained for GOE random matrices. Most error bars in panels (e)-(h) are smaller than the symbols.

The decay of the survival probability is controlled by $b_1^2(\Gamma t)$, which at the time $t_m \propto D^{2/3}/\Gamma$ meets the b_2 function at the minimum value of the survival probability, $\sim 2/D$. After this point, the evolution is described entirely by the b_2 function, which brings $\langle P_S(t) \rangle$ from its minimum up to the saturation value at $\sim 3/D$. Saturation happens at the Heisenberg time $t_H \propto D/\Gamma$.

The time interval governed by the b_2 function, where $\langle P_S(t) \rangle < \langle \overline{P_S} \rangle$, is known as correlation hole [35–42] or “ramp” [43–45]. It is a dynamical manifestation of spectral correlations, and, therefore, a dynamical signature of quantum chaos. The point in time where the ramp starts, t_m , has been referred to as Thouless time [35, 65]. It coincides with the time where the inverse participation ratio reaches its minimum value [35], indicating that t_m is the time that it takes for the initial state to maximally spread over the many-body Hilbert space and acquire weight over the unperturbed many-body states $|\phi_n\rangle$ in its microcanonical energy shell given by the width Γ .

The evolution of the mean survival probability for the spin model (1) is shown in Fig. 1 (a) for different system sizes. There is an excellent agreement between the numerical results and expression (8) when $W = 0.5$, which corresponds to the deep chaotic regime. The correlation hole is evident in all the curves and it does not fade away as L increases. This means that the complete equilibration of this quantity takes place only after the hole ends at the Heisenberg time t_H . Since this time is exponentially long in the system size L , we use exact diagonalization to resolve the entire dynamics, which limits the accessible systems sizes to $L = 18$.

A correlation hole is also visible for the spin autocorrelation function, as depicted in Fig. 1 (c), suggesting that for sufficiently small system sizes, where it develops for times that are not exceedingly long and reaches minimum values that are not too small, the hole might be experimentally detected.

In contrast to the survival probability and the spin autocorrelation function, the effects of the spectral correlations in the evolution of $\langle I_{PR}(t) \rangle$ [Fig. 1 (b)] and of $\langle C(t) \rangle$ [Fig. 1 (d)] are minor and the correlation hole is hardly discernible. Furthermore, for $\langle I_{PR}(t) \rangle$, $\langle C(t) \rangle$, and also $\langle \mathcal{I}(t) \rangle$, the hole gets smaller as the system size increases, which justifies neglecting it in the definition of the thermalization time for these quantities.

The relative depth of the correlation hole for a given observable \hat{O} can be measured by the ratio [41, 66, 67]

$$\kappa = \frac{\langle \overline{O} \rangle - \langle O \rangle_{\min}}{\langle \overline{O} \rangle}, \quad (12)$$

where $\langle O \rangle_{\min}$ stands for the value of the observable at the minimum of the correlation hole. For the survival probability, κ converges to a constant, while it decreases with system size for the other quantities.

When the survival probability is evolved using full random matrices taken from a Gaussian orthogonal ensemble (GOE), it is known analytically that $\langle \overline{P_S} \rangle \sim 3/D$ and $\langle P_S \rangle_{\min} \sim 2/D$ [35, 39], which yields $\kappa = 1/3$. In Fig. 1 (e), we show κ for the survival probability of the spin model as a function of system size for different disorder strengths

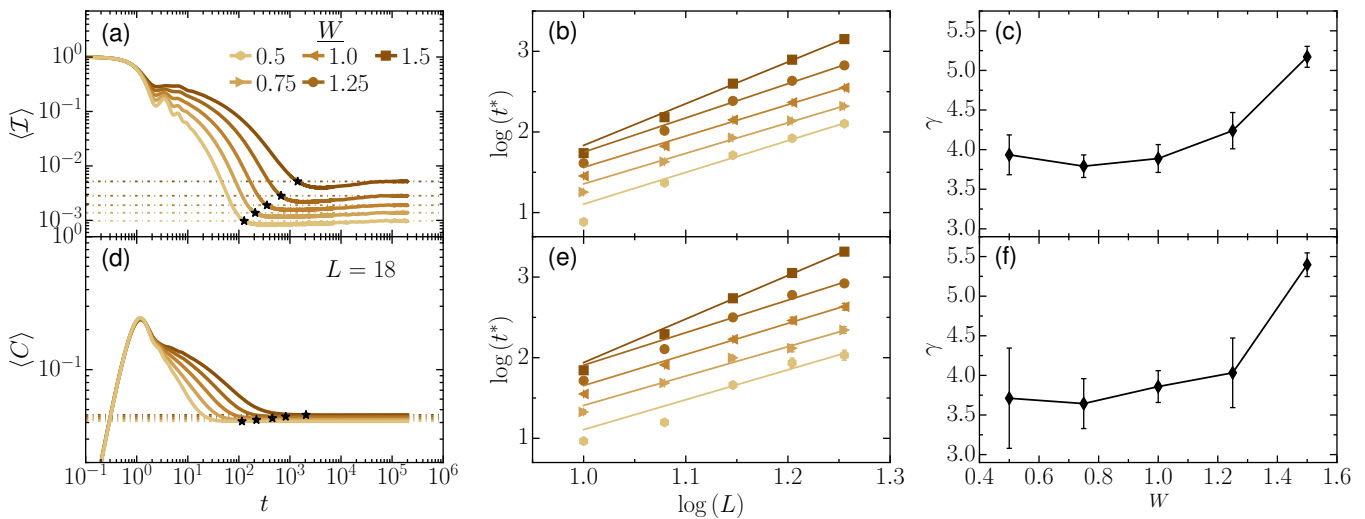


FIG. 2. *Upper [Lower] panels*: Analysis of the crossing time for the spin autocorrelation function $\langle \mathcal{I}(t) \rangle$ [connected spin-spin autocorrelation function $\langle C(t) \rangle$]. (a) [(d)] Evolution of the mean spin autocorrelation function [connected spin-spin autocorrelation function] for $L = 18$. Each curve corresponds to a different disorder strength W , as indicated. The horizontal dotted-dashed lines represent the asymptotic value of the observable and the crossing time t^* is marked with a star. (b) [(e)] Scaling of the crossing time t^* with L . Symbols are the data and solid lines give power-law fits to $t^* \propto L^\gamma$. Error bars indicate the standard deviation of the bootstrap procedure. (c) [(f)] Exponent γ extracted from the power-law fit to the data points in (b) [(e)] as a function of W . Error bars indicate the standard deviation on the fitted exponent.

in the chaotic regime. The relative depth clearly converges to $\kappa = 1/3$, which is indicated with a horizontal dashed line. The correlation hole is therefore a robust property of the survival probability.

Contrary to the survival probability, the relative depth κ for $\langle \text{IPR}(t) \rangle$ [Fig. 1 (f)], $\langle \mathcal{I}(t) \rangle$ [Fig. 1 (g)], and $\langle C(t) \rangle$ [Fig. 1 (h)] decays with L . In the case of the inverse participation ratio and the connected spin-spin correlation function, the decay is exponential, while for the spin autocorrelation function, the results are more subtle and make apparent the danger of finite-size effects. While for $W = 0.5$, κ decreases monotonically with L , for $W = 0.75$ and $W = 1$, κ increases for small values of L and the decay becomes clear only for $L > 14$.

IV. THERMALIZATION BEFORE THE CORRELATION HOLE

Ignoring the correlation hole, we define the thermalization time as the point where $\langle \hat{O}(t) \rangle$ first crosses the infinite-time average $\langle \bar{O} \rangle$. We denote this time by t^* , which is clearly much smaller than the Heisenberg time, $t^* \ll t_H$. These crossing points are marked with stars in Figs. 1 (a)-(d).

A. Weak disorder region: $0.5 \leq W \leq 1$

For sufficiently weak disorder, $W = 0.5$ [68], we can make use of the semi-analytical expression in Eq. (8) to estimate the dependence of t^* on system size. At long times, disregarding the correlation hole, the decay of $\langle P_S(t) \rangle$ is given by [69, 70]

$$\langle P_S(t \gg \Gamma^{-1}) \rangle_{\text{decay}} \simeq \frac{e^{-E_{\text{max}}^2/\Gamma^2} + e^{-E_{\text{min}}^2/\Gamma^2}}{2\pi\mathcal{N}^2\Gamma^2 t^2}. \quad (13)$$

Using that E_{min} , E_{max} and Γ^2 are extensive, namely proportional to the size of the system, and that the survival probability saturates at $\langle \bar{P}_S \rangle \sim 3/D$, we find that $t^* \propto \exp(0.22L)$, which agrees very well with the crossing time obtained numerically for $L = 10, 12, 14, 16, 18, 20, 22$. Knowing the saturation value of the survival probability, we can evolve $|\Psi(t)\rangle$ up to a vicinity of t^* only, which is a major saving compared to the evolution up to t_H . This allows us to use Krylov-space methods for the time evolution of the survival probability and access to system sizes $L > 18$. For the seven system sizes considered, we verified that the exponential scaling of t^* with L is indeed better than a power-law scaling.

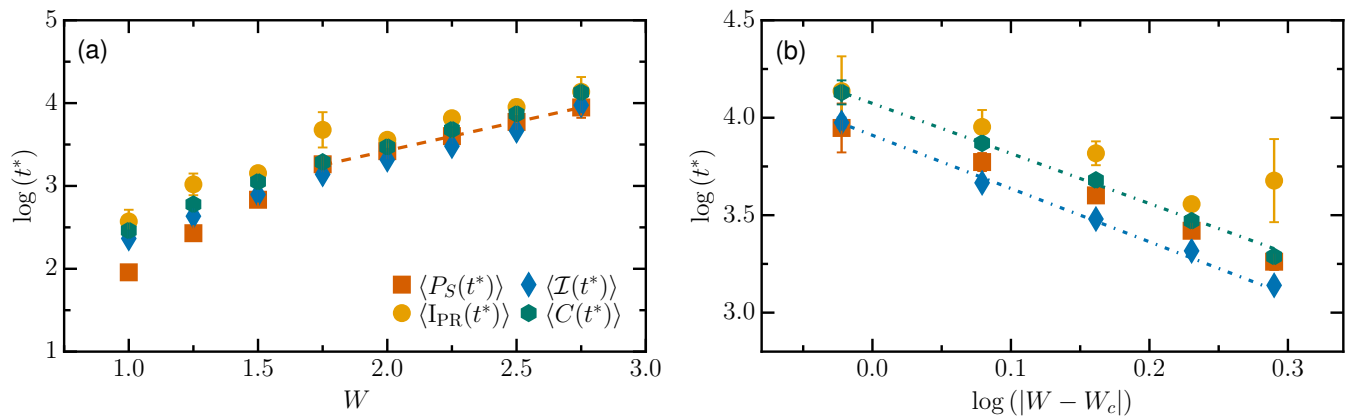


FIG. 3. Dependence of the crossing time t^* on (a) [(b)] the disorder strength W [the difference $|W - W_c|$; with $W_c = 3.7$] for the survival probability $\langle P_S(t) \rangle$, inverse participation ratio $\langle I_{\text{PR}}(t) \rangle$, spin autocorrelation function $\langle \mathcal{I}(t) \rangle$, and the connected spin-spin correlation function $\langle C(t) \rangle$ for system size $L = 16$. The symbols representing each quantity are shown in panel (a). The dashed [dotted-dashed] lines in (a) [(b)] correspond to exponential [power-law] fits obtained with the points for $W \geq 1.75$. Error bars indicate the standard deviation of the bootstrap procedure.

While an analytical expression is not available for the time-dependence of the inverse participation ratio, in the weak disorder regime, its saturation value is known analytically, $\langle \overline{I_{\text{PR}}} \rangle \sim 2/D$ [71], so we can also obtain t^* for system sizes $L > 18$. To do that, we apply a Savitzky-Golay filter to smooth the curves for $\langle I_{\text{PR}}(t) \rangle$ and then extract the crossing time [72]. For this quantity, we find that a power-law scaling of t^* with L actually works better than an exponential scaling. This makes us suspect that the exponential dependence of the crossing time with system size found for the survival probability may be related to the prevalence of the correlation hole, a conjecture that is further reinforced by the next results.

For the two local quantities, we do not have analytical results for the saturation values, hence our analysis is restricted to five system sizes. In Fig. 2 (a) and Fig. 2 (d), we fix the system size at $L = 18$ and mark the crossing time for the curves of $\langle \mathcal{I}(t) \rangle$ and $\langle C(t) \rangle$ obtained for different disorder strengths. In Fig. 2 (b) and Fig. 2 (e), we present the scaling analysis for both quantities and those values of W . We find that, similarly to the inverse participation ratio, the dependence of t^* with L is better fitted with a power law than an exponential, that is

$$t^* \propto L^\gamma \quad \text{with} \quad \gamma > 3. \quad (14)$$

The exact value of the exponent γ varies with the disorder strength, as shown in Fig. 2 (c) and Fig. 2 (f). For disorder strength $0.5 \leq W \leq 1$, we find that on average $\gamma \approx 3.8 \pm 0.3$. The value of the exponent is somewhat close to that argued in [28, 73], but larger than the value which typically appears in studies of transport behavior [31, 34].

B. Near critical region: $1 < W < W_c$

Figure 2 shows the crossing time t^* of the local quantities computed for disorder strengths slightly larger than the coupling parameter, $W \gtrsim J$. The power-law fit is still better than the exponential one, although γ [Eq. (14)] for $W = 1.5$ is larger than 5, as seen in Fig. 2 (c) and Fig. 2 (f). The scaling analysis of the crossing time for $W > 1$ is more difficult, because in this region, the use of random matrices for guidance is no longer justified and longer propagation times are typically required to obtain thermalization. We leave open the question of whether the scaling remains power law with even larger exponents or becomes exponential as the critical point is approached (see related discussions in [27, 31]). In the following, we analyze how the crossing time t^* depends on the disorder strength for a fixed L .

It was shown that the time for the minimum of the correlation hole, t_m , for the survival probability and for the spin autocorrelation function grows exponentially as the disorder strength increases [35], which was later confirmed in terms of a spectral analysis [65]. It is thus relevant to examine the dependence of t^* on W , which we do in Fig. 3. The behavior of the crossing time t_* is not conclusive as can be seen from Fig. 3. Considering disorder strengths $W \in [1, 3]$, the time t^* is best fitted with a stretched exponential, but if we consider disorder strengths closer to the critical point, $W \geq 1.75$, we see that either an exponential dependence $t^* \propto \exp(W/W')$ or a critical form $t^* \propto |W - W_c|^{-\beta}$ with an exponent $\beta \approx 2.6 \pm 0.08$ describe the data reasonably well for all the quantities, except for the inverse participation

ratio, which exhibits strong fluctuations in its corresponding crossing times. The quality of the fits varies depending on the quantity: the survival probability is better described by an exponential form [Fig. 3 (a)], while the local quantities seem to have critical scaling [Fig. 3 (b)]. We did not see a qualitative change in our conclusions when varying W_c from 3.5 to 6.

V. CONCLUSIONS

We investigated how the thermalization time of the disordered spin-1/2 Heisenberg chain depends on the system size L for four different observables. If the correlation hole is taken into account when defining the thermalization time, then it coincides with the Heisenberg time and thus grows exponentially with L . This is what happens for the survival probability, where the correlation hole persists in the thermodynamic limit. However, for the inverse participation ratio, spin autocorrelation function, and connected spin-spin correlation function, the correlation hole fades away as L increases, which justifies neglecting it. In this case, we defined the thermalization time as the point where the evolution of the observables first crosses their infinite-time averages. The dependence of this crossing time on system size is best described by a power law.

Chaotic systems with static Hamiltonians conserve at least the total energy, have diffusive energy transport, and their thermalization time, namely the time it takes for a non-uniformity in the energy density to spread across the system, is expected to be bounded from below by L^2 . For disordered chaotic systems transport is expected to be subdiffusive [18, 19, 24, 29, 58], and their thermalization time to be bounded from below by L^γ with $\gamma > 2$, though for very weak disorder, γ is expected to approach the lower bound, $\gamma \approx 2$, where transport is indistinguishable from diffusion. Interestingly, even for the lowest disorder that we study, $W \approx 0.5$, the thermalization time scales as L^γ with $\gamma > 3$, so it is parametrically larger than the time it takes to make the energy density homogeneous. We leave for future studies the question of how the system is away from thermal equilibrium during the times $L^2 < t < L^3$.

We have provided a brief analysis of the dependence of the crossing time t^* on the disorder strength away from the critical point. Although it is hard to discern between an exponentially growing t^* with W and a critical behavior $t^* \propto |W - W_c|^{-\beta}$, the survival probability seems to be better described by the former, while the local quantities appear to show the critical scaling with an exponent $\beta \approx 2.6$.

In summary, by analyzing the evolution of experimentally measurable observables up to thermalization in a paradigmatic many-body quantum system, we were able to identify the thermalization time without any assumptions or approximations. We have seen that the thermalization time grows exponentially with the system size for the survival probability, but only as a power law for quantities which are local in real space. It is to be determined whether this apparent difference in the scaling is related to the vanishing of the correlation hole in the thermodynamic limit, which we also leave for future studies.

ACKNOWLEDGMENTS

This research was supported by a grant from the United States-Israel Binational Foundation (BSF, Grant No. 2019644), Jerusalem, Israel, and the United States National Science Foundation (NSF, Grant No. DMR-1936006). T.L.M.L. acknowledges funding from the Kreitman fellowship. E.J.T.-H. is grateful to LNS-BUAP for their supercomputing facility. Computing resources supporting this work were provided by the CEAFCM and Universidad de Huelva High Performance Computer (HPC@UHU) located in the Campus Universitario el Carmen and funded by FEDER/MINECO project UNHU-15CE-2848. F.P.B. thanks Spanish National Research, Development, and Innovation plan (RDI plan) under the project PID2019-104002GB-C21 and the Consejería de Conocimiento, Investigación y Universidad, Junta de Andalucía and European Regional Development Fund (ERDF), refs. SOMM17/6105/UGR and UHU-1262561.

-
- [1] A. Peres, Stability of quantum motion in chaotic and regular systems, *Phys. Rev. A* **30**, 1610 (1984).
 - [2] H. Tasaki, From quantum dynamics to the canonical distribution: General picture and a rigorous example, *Phys. Rev. Lett.* **80**, 1373 (1998).
 - [3] P. Reimann, Foundation of statistical mechanics under experimentally realistic conditions, *Phys. Rev. Lett.* **101**, 190403 (2008).
 - [4] A. J. Short, Equilibration of quantum systems and subsystems, *New J. Phys.* **13**, 053009 (2011).
 - [5] P. R. Zangara, A. D. Dente, E. J. Torres-Herrera, H. M. Pastawski, A. Iucci, and L. F. Santos, Time fluctuations in isolated quantum systems of interacting particles, *Phys. Rev. E* **88**, 032913 (2013).

- [6] T. Kiendl and F. Marquardt, Many-particle dephasing after a quench, *Phys. Rev. Lett.* **118**, 130601 (2017).
- [7] S. Goldstein, T. Hara, and H. Tasaki, Time scales in the approach to equilibrium of macroscopic quantum systems, *Phys. Rev. Lett.* **111**, 140401 (2013).
- [8] S. Goldstein, T. Hara, and H. Tasaki, Extremely quick thermalization in a macroscopic quantum system for a typical nonequilibrium subspace, *New J. Phys.* **17**, 045002 (2015).
- [9] T. R. de Oliveira, C. Charalambous, D. Jonathan, M. Lewenstein, and A. Riera, Equilibration time scales in closed many-body quantum systems, *New J. Phys.* **20**, 033032 (2018).
- [10] P. Reimann and M. Kastner, Equilibration of isolated macroscopic quantum systems, *New J. Phys.* **14**, 043020 (2012).
- [11] P. Reimann, Typical fast thermalization processes in closed many-body systems, *Nat. Commun.* **7**, 10821 (2016).
- [12] A. J. Short and T. C. Farrelly, Quantum equilibration in finite time, *New J. Phys.* **14**, 013063 (2012).
- [13] T. Monnai, Generic evaluation of relaxation time for quantum many-body systems: Analysis of the system size dependence, *J. Phys. Soc. Jpn.* **82**, 044006 (2013).
- [14] D. Hetterich, M. Fuchs, and B. Trauzettel, Equilibration in closed quantum systems: Application to spin qubits, *Phys. Rev. B* **92**, 155314 (2015).
- [15] C. Gogolin and J. Eisert, Equilibration, thermalisation, and the emergence of statistical mechanics in closed quantum systems, *Rep. Prog. Phys.* **79**, 056001 (2016).
- [16] L. P. García-Pintos, N. Linden, A. S. L. Malabarba, A. J. Short, and A. Winter, Equilibration time scales of physically relevant observables, *Phys. Rev. X* **7**, 031027 (2017).
- [17] A. S. L. Malabarba, L. P. García-Pintos, N. Linden, T. C. Farrelly, and A. J. Short, Quantum systems equilibrate rapidly for most observables, *Phys. Rev. E* **90**, 012121 (2014).
- [18] Y. Bar Lev, G. Cohen, and D. R. Reichman, Absence of diffusion in an interacting system of spinless fermions on a one-dimensional disordered lattice, *Phys. Rev. Lett.* **114**, 100601 (2015).
- [19] K. Agarwal, S. Gopalakrishnan, M. Knap, M. Müller, and E. Demler, Anomalous diffusion and griffiths effects near the many-body localization transition, *Phys. Rev. Lett.* **114**, 160401 (2015).
- [20] A. C. Potter, R. Vasseur, and S. A. Parameswaran, Universal properties of many-body delocalization transitions, *Phys. Rev. X* **5**, 031033 (2015).
- [21] R. Vosk, D. A. Huse, and E. Altman, Theory of the many-body localization transition in one-dimensional systems, *Phys. Rev. X* **5**, 031032 (2015).
- [22] M. Serbyn, Z. Papić, and D. A. Abanin, Criterion for many-body localization-delocalization phase transition, *Phys. Rev. X* **5**, 041047 (2015).
- [23] M. Žnidarič, A. Scardicchio, and V. K. Varma, Diffusive and subdiffusive spin transport in the ergodic phase of a many-body localizable system, *Phys. Rev. Lett.* **117**, 040601 (2016).
- [24] D. J. Luitz, N. Laflorencie, and F. Alet, Extended slow dynamical regime close to the many-body localization transition, *Phys. Rev. B* **93**, 060201 (2016).
- [25] D. J. Luitz and Y. Bar Lev, Anomalous thermalization in ergodic systems, *Phys. Rev. Lett.* **117**, 170404 (2016).
- [26] S. Bera, G. De Tomasi, F. Weiner, and F. Evers, Density propagator for many-body localization: Finite-size effects, transient subdiffusion, and exponential decay, *Phys. Rev. Lett.* **118**, 196801 (2017).
- [27] M. Serbyn, Z. Papić, and D. A. Abanin, Thouless energy and multifractality across the many-body localization transition, *Phys. Rev. B* **96**, 104201 (2017).
- [28] A. Dymarsky, Bound on eigenstate thermalization from transport, (2018), [arXiv:1804.08626 \[cond-mat.stat-mech\]](https://arxiv.org/abs/1804.08626).
- [29] D. J. Luitz and Y. Bar Lev, The ergodic side of the many-body localization transition, *Ann. Phys.* **529**, 1600350 (2017).
- [30] B. Bertini, F. Heidrich-Meisner, C. Karrasch, T. Prosen, R. Steinigeweg, and M. Žnidarič, Finite-temperature transport in one-dimensional quantum lattice models, (2020), [arXiv:2003.03334 \[cond-mat.str-el\]](https://arxiv.org/abs/2003.03334).
- [31] S. Gopalakrishnan and S. Parameswaran, Dynamics and transport at the threshold of many-body localization, *Phys. Rep.* **862**, 1 (2020).
- [32] V. Zelevinsky, B. A. Brown, N. Frazier, and M. Horoi, The nuclear shell model as a testing ground for many-body quantum chaos, *Phys. Rep.* **276**, 85 (1996).
- [33] F. Borgonovi, F. Izrailev, L. Santos, and V. Zelevinsky, Quantum chaos and thermalization in isolated systems of interacting particles, *Phys. Rep.* **626**, 1 (2016).
- [34] L. D'Alessio, Y. Kafri, A. Polkovnikov, and M. Rigol, From quantum chaos and eigenstate thermalization to statistical mechanics and thermodynamics, *Adv. Phys.* **65**, 239 (2016).
- [35] M. Schiulaz, E. J. Torres-Herrera, and L. F. Santos, Thouless and relaxation time scales in many-body quantum systems, *Phys. Rev. B* **99**, 174313 (2019).
- [36] L. Leviandier, M. Lombardi, R. Jost, and J. P. Pique, Fourier transform: A tool to measure statistical level properties in very complex spectra, *Phys. Rev. Lett.* **56**, 2449 (1986).
- [37] T. Guhr and H. Weidenmüller, Correlations in anticrossing spectra and scattering theory. analytical aspects, *Chem. Phys.* **146**, 21 (1990).
- [38] J. Wilkie and P. Brumer, Time-dependent manifestations of quantum chaos, *Phys. Rev. Lett.* **67**, 1185 (1991).
- [39] Y. Alhassid and R. D. Levine, Spectral autocorrelation function in the statistical theory of energy levels, *Phys. Rev. A* **46**, 4650 (1992).
- [40] T. Gorin and T. H. Seligman, Signatures of the correlation hole in total and partial cross sections, *Phys. Rev. E* **65**, 026214 (2002).
- [41] E. Torres-Herrera and L. F. Santos, Dynamical manifestations of quantum chaos: correlation hole and bulge, *Philos. Trans. R. Soc. London, Ser. A* **375**, 20160434 (2017).

- [42] E. J. Torres-Herrera, A. M. García-García, and L. F. Santos, Generic dynamical features of quenched interacting quantum systems: Survival probability, density imbalance, and out-of-time-ordered correlator, *Phys. Rev. B* **97**, 060303 (2018).
- [43] J. Cotler, N. Hunter-Jones, J. Liu, and B. Yoshida, Chaos, complexity, and random matrices, *J. High Energy Phys.* **2017** (11), 48.
- [44] H. Gharibyan, M. Hanada, S. H. Shenker, and M. Tezuka, Onset of random matrix behavior in scrambling systems, *J. High Energy Phys.* **2018** (7), 124.
- [45] M. Winer and B. Swingle, Hydrodynamic theory of the connected spectral form factor (2020), arXiv:2012.01436.
- [46] S. Gherardini, C. Lovecchio, M. M. Müller, P. Lombardi, F. Caruso, and F. S. Cataliotti, Ergodicity in randomly perturbed quantum systems, *Quantum Sci. Technol.* **2**, 015007 (2017).
- [47] K. Singh, C. J. Fujiwara, Z. A. Geiger, E. Q. Simmons, M. Lipatov, A. Cao, P. Dotti, S. V. Rajagopal, R. Senaratne, T. Shimasaki, M. Heyl, A. Eckardt, and D. M. Weld, Quantifying and controlling prethermal nonergodicity in interacting floquet matter, *Phys. Rev. X* **9**, 041021 (2019).
- [48] M. Schreiber, S. S. Hodgman, P. Bordia, H. P. Lüschen, M. H. Fischer, R. Vosk, E. Altman, U. Schneider, and I. Bloch, Observation of many-body localization of interacting fermions in a quasirandom optical lattice, *Science* **349**, 842 (2015).
- [49] P. Richerme, Z.-X. Gong, A. Lee, C. Senko, J. Smith, M. Foss-Feig, S. Michalakis, A. V. Gorshkov, and C. Monroe, Non-local propagation of correlations in quantum systems with long-range interactions, *Nature* **511**, 198 (2014).
- [50] L. F. Santos, G. Rigolin, and C. O. Escobar, Entanglement versus chaos in disordered spin chains, *Phys. Rev. A* **69**, 042304 (2004).
- [51] R. Nandkishore and D. A. Huse, Many-body localization and thermalization in quantum statistical mechanics, *Annu. Rev. Condens. Matter Phys.* **6**, 15 (2015).
- [52] F. Alet and N. Laflorencie, Many-body localization: An introduction and selected topics, *C. R. Phys.* **19**, 498 (2018).
- [53] D. A. Abanin, E. Altman, I. Bloch, and M. Serbyn, Colloquium: Many-body localization, thermalization, and entanglement, *Rev. Mod. Phys.* **91**, 021001 (2019).
- [54] V. Oganesyan and D. A. Huse, Localization of interacting fermions at high temperature, *Phys. Rev. B* **75**, 155111 (2007).
- [55] A. Pal and D. A. Huse, Many-body localization phase transition, *Phys. Rev. B* **82**, 174411 (2010).
- [56] T. C. Berkelbach and D. R. Reichman, Conductivity of disordered quantum lattice models at infinite temperature: Many-body localization, *Phys. Rev. B* **81**, 224429 (2010).
- [57] J. A. Kjäll, J. H. Bardarson, and F. Pollmann, Many-Body Localization in a Disordered Quantum Ising Chain, *Phys. Rev. Lett.* **113**, 107204 (2014).
- [58] Y. Bar Lev and D. R. Reichman, Dynamics of many-body localization, *Phys. Rev. B* **89**, 220201 (2014).
- [59] D. J. Luitz, N. Laflorencie, and F. Alet, Many-body localization edge in the random-field Heisenberg chain, *Phys. Rev. B* **91**, 081103(R) (2015).
- [60] T. Devakul and R. R. P. Singh, Early breakdown of area-law entanglement at the many-body delocalization transition, *Phys. Rev. Lett.* **115**, 187201 (2015).
- [61] E. V. H. Doggen, F. Schindler, K. S. Tikhonov, A. D. Mirlin, T. Neupert, D. G. Polyakov, and I. V. Gornyi, Many-body localization and delocalization in large quantum chains, *Phys. Rev. B* **98**, 174202 (2018).
- [62] L. Herviou, S. Bera, and J. H. Bardarson, Multiscale entanglement clusters at the many-body localization phase transition, *Phys. Rev. B* **99**, 134205 (2019).
- [63] D. Abanin, J. Bardarson, G. De Tomasi, S. Gopalakrishnan, V. Khemani, S. Parameswaran, F. Pollmann, A. Potter, M. Serbyn, and R. Vasseur, Distinguishing localization from chaos: Challenges in finite-size systems, *Annals of Physics* , 168415 (2021).
- [64] M. L. Mehta, *Random Matrices* (Academic Press, Boston, USA, 1991).
- [65] J. Šuntajs, J. Bonča, T. Prosen, and L. Vidmar, Quantum chaos challenges many-body localization (2020), arXiv:1905.06345 [cond-mat.str-el].
- [66] E. J. Torres-Herrera and L. F. Santos, Extended nonergodic states in disordered many-body quantum systems, *Annalen der Physik* **529**, 1600284 (2017).
- [67] E. J. Torres-Herrera and L. F. Santos, Signatures of chaos and thermalization in the dynamics of many-body quantum systems, *Eur. Phys. J. Spec. Top.* **227**, 1897 (2019).
- [68] Since for $W = 0$ the system is integrable, the disorder cannot be too small.
- [69] M. Távora, E. J. Torres-Herrera, and L. F. Santos, Inevitable power-law behavior of isolated many-body quantum systems and how it anticipates thermalization, *Phys. Rev. A* **94**, 041603 R (2016).
- [70] M. Távora, E. J. Torres-Herrera, and L. F. Santos, Power-law decay exponents: A dynamical criterion for predicting thermalization, *Phys. Rev. A* **95**, 013604 (2017).
- [71] E. J. Torres-Herrera, I. Vallejo-Fabila, A. J. Martínez-Mendoza, and L. F. Santos, Self-averaging in many-body quantum systems out of equilibrium: Time dependence of distributions, *Phys. Rev. E* **102**, 062126 (2020).
- [72] The statistical errors of this procedure were accounted for using a bootstrapping procedure with 1000 bootstrap samples, each composed of $N = 9000$ random samples taken from the full random data set of over 10^4 elements.
- [73] J. Richter, A. Dymarsky, R. Steinigeweg, and J. Gemmer, Eigenstate thermalization hypothesis beyond standard indicators: Emergence of random-matrix behavior at small frequencies, *Phys. Rev. E* **102**, 042127 (2020).